Temporal Discharge Patterns Evoked by Rapid Sequences of Wide- and Narrowband Clicks in the Primary Auditory Cortex of Cat

THOMAS LU AND XIAOQIN WANG
Laboratory of Auditory Neurophysiology, Department of Biomedical Engineering, Johns Hopkins University School of Medicine, Baltimore, Maryland 21205

Received 14 October 1999; accepted in final form 10 April 2000

Lu, Thomas and Xiaoqin Wang. Temporal discharge patterns evoked by rapid sequences of wide- and narrowband clicks in the primary auditory cortex of cat. *J Neurophysiol* 84: 236–246, 2000. The present study investigated neural responses to rapid, repetitive stimuli in the primary auditory cortex (A1) of cats. We focused on two important issues regarding cortical coding of sequences of stimuli: temporal discharge patterns of A1 neurons as a function of interstimulus interval and cortical mechanisms for representing successive stimulus events separated by very short intervals. These issues were studied using wide- and narrowband click trains with inter-click intervals (ICIs) ranging from 3 to 100 ms as a class of representative sequential stimuli. The main findings of this study are *1*) A1 units displayed, in response to click train stimuli, three distinct temporal discharge patterns that we classify as regions I, II, and III. At long ICIs nearly all A1 units exhibited typical stimulus-synchronized response patterns (region I) consistent with previously reported observations. At intermediate ICIs, no clear temporal structures were visible in the responses of most A1 units (region II). At short ICIs, temporal discharge patterns are characterized by the presence of either intrinsic oscillations (at ~10 Hz) or a change in discharge rate that was a monotonically decreasing function of ICI (region III). In some A1 units, temporal discharge patterns corresponding to region III were absent. *2*) The boundary between regions I and II (*synchronization boundary*) had a median value of 39.8 ms ICI ([25%, 75%] = [20.4, 58.8] ms ICI; $n = 131$). The median boundary between regions II and III was estimated at 6.3 ms ([25%, 75%] = [5.2, 9.7] ms ICI; $n = 47$) for units showing rate changes (*rate-change boundary*). *3*) The boundary values between different regions appeared to be relatively independent of stimulus intensity (at modest sound levels) or the bandwidth of the clicks used. *4*) There is a weak correlation between a unit's synchronization boundary and its response latency. Units with shorter latencies appeared to also have smaller boundary values. And *5*) based on these findings, we proposed a two-stage model for A1 neurons to represent a wide range of ICIs. In this model, A1 uses a temporal code for explicitly representing long ICIs and a rate code for implicitly representing short ICIs.

INTRODUCTION

Time-varying features of acoustic signals and their neural representations in the cortex are of special interest to our understanding of complex sound processing at this level of the auditory system. Temporal features are fundamental components of communication sounds such as human speech and animal vocalizations. Both humans and animals are capable of perceiving very rapidly changing components in complex sounds. It has long been known that, unlike at the auditory periphery, neurons in the auditory cortex do not faithfully follow such rapidly changing stimulus components (see review, Langner 1992). Cortical neurons have only limited stimulus-synchronization capacity. It is of great importance to know what is this limit for neurons in the auditory cortex and, furthermore, how the auditory cortex represents rapidly changing stimulus components beyond this limitation. In the present study, we attempted to shed light on these questions by studying neural responses in the primary auditory cortex (A1) of cats to repetitive stimulus events using click train stimuli.

Clicks have been widely used in perceptual studies to determine the limits of temporal information processing by the auditory system because of their brief duration and easiness to implement. Ronken (1970) found that humans could discriminate between time-reversed pairs of clicks (2 250-μs clicks of unequal amplitude) with an inter-click interval as small as 2 ms. A similar temporal limit can also be demonstrated by gap detection tasks between two noise bursts (Plomp 1964). Detection of extremely fine gaps of 1–20 μs in high-frequency pulse trains has been reported, although the perceptual task may have relied to some extent on spectral cues (Pollack 1967, 1968). The actual discrimination performance by humans in these studies is much better than what would be predicted from neuronal activity observed in the auditory cortex.

While the preceding studies demonstrate fine discrimination ability, other studies have looked at the perceptual quality of successive stimuli. Miller and Taylor (1948) examined the question of continuousness versus discreteness in repeated noise gap stimuli. They found that the rate of interruptions (gaps) in their noise stimuli needed to be at least 10–15 Hz before the perception of each noise burst in the stimuli begin to fuse and 40–250 Hz for a pitch to arise. Hirsch (1959) showed that perception of two distinct successive stimuli requires at least 15–20 ms of separation. This was also seen in magnetoencephalographic recordings (Joliot et al. 1994). These data provide motivation for our neurophysiological studies.

Although perceptual studies have shown that humans can detect temporal features on short time scales, existing neurophysiological studies of the auditory cortex have revealed no direct neural correlates. There have been a number of studies in

Address for reprint requests: X. Wang, Dept. of Biomedical Engineering, Johns Hopkins University School of Medicine, 720 Rutland Ave., Ross 424, Baltimore, MD 21205 (E-mail: xwang@bme.jhu.edu).

The costs of publication of this article were defrayed in part by the payment of page charges. The article must therefore be hereby marked "*advertisement*" in accordance with 18 U.S.C. Section 1734 solely to indicate this fact.

the past using clicks or other temporally modulated stimuli to probe the temporal resolution of A1 neurons (Bieser and Muller-Preuss 1996; Creutzfeldt et al. 1980; de Ribaupierre et al. 1972; Eggermont 1991, 1992, 1994, 1998, 1999; Erulkar et al. 1956; Gaese and Ostwald 1995; Goldstein et al. 1959; Phillips et al. 1989; Schreiner and Urbas 1988; Steinschneider et al. 1980; Whitfield and Evans 1965). Some of the earliest studies using click stimuli to investigate limiting rate of stimulus-synchronized temporal discharges in the auditory cortex were done in unanesthetized cats (de Ribaupierre et al. 1972; Goldstein et al. 1959). de Ribaupierre et al. (1972) showed that there was a broad range of stimulus-synchronized responses to click trains in a cat's auditory cortex, with a median value between 50 and 100 Hz (repetition frequency of clicks). Creutzfeldt et al. (1980) demonstrated large reductions in stimulus-following responses from thalamus to cortex in unanesthetized guinea pigs. Their cortical responses tended to be transient and entrainment occurred only when the modulation rate was $<$20 Hz, even though a correlated thalamic neuron responded with stimulus-synchronized discharges up to 200 Hz. Phillips et al. (1989) recorded the responses of auditory cortex neurons from anesthetized cat in response to repetitive tone pulses and found that stimulus-synchronized frequencies reached no more than 10 Hz. The mechanism of limited stimulus-synchronization was hypothesized to be the result of a suppression period of 130–135 ms immediately after each click, followed by a rebound in the neuron's discharge rate (Eggermont 1992).

The objectives of most previous studies using click trains or amplitude-modulated (AM) tones have been to define modulation transfer functions (MTFs) of A1 neurons (see review by Langner 1992). They focused largely on processing of stimulus intervals in the order of tens and hundreds of milliseconds since MTFs typically peak at 8–10 Hz (equivalent to inter-stimulus intervals of 100–125 ms) in anesthetized cortex. At higher repetition rates (or shorter inter-stimulus intervals), A1 neurons are either not stimulus-synchronized to the individual stimuli or not responsive altogether. In contrast, MTFs of auditory-nerve fibers are low-pass in nature and have cutoff frequencies near ~1 kHz (Joris and Yin 1992; Palmer 1982). At the level of the auditory cortex, few studies have investigated neural responses to rapidly modulated sequential stimuli in the order of a few milliseconds to tens of milliseconds. Such data are especially valuable to understand the discrepancy between the missing temporal information at the cortex corresponding to rapid successive stimuli and the perceptibility of such stimuli by humans and animals.

The objectives of the present study are twofold: to quantitatively define inter-click interval (ICI) boundaries below which A1 neurons are no longer stimulus-synchronized or no longer responsive to click train stimuli and to search for evidence that A1 neurons can implicitly encode shorter ICIs by a rate code instead of an explicit temporal code, such as suggested in Bieser and Muller-Preuss (1996). In the experiments reported here, we focused on cortical responses to click trains with ICIs shorter than 100 ms in populations of A1 units. The results of this study showed that A1 units exhibit three types of distinct temporal discharge patterns at different ICIs: stimulus-synchronized, rate-change, and oscillation. Based on our findings, we suggested a two-stage model for the auditory cortex to represent ICIs across all ranges.

METHODS

Animal preparation

Adult cats with healthy and infection-free ears were used. Initially, ketamine (30 mg/kg), xylazine (3 mg/kg), and atropine sulfate (0.03 mg/kg) were administered intramuscularly. Pentobarbital sodium (3 $mg \cdot kg^{-1} \cdot h^{-1}$ iv) or ketamine (6.7 mg/kg im), and a 1:9 volume mix (0.25 ml/kg) of acepromazine (0.25 mg/ml) and atropine (5 mg/ml) were periodically administered as needed throughout an experiment to maintain an animal at an areflexic level. Core body temperature of 38°C was maintained and monitored by a heating pad and rectal thermometer. Local anesthetic (lidocaine) was used before any soft-tissue incision during surgery. The cats were cannulated through either the cephalic or the saphenous vein, and a tracheotomy was performed to allow unobstructed breathing. The cats were then placed into a head holder. A sagittal incision was made over the left hemisphere, and the skin was reflected. Underneath, the temporalis and frontalis muscles were retracted to expose the skull underneath. The location of the primary auditory cortex was estimated to be 1/3 distance from the frontal ridge to the occipital ridge and the same distance from the midline. A 1-cm^2 area of the skull was removed, and the dura was reflected to expose the cortical surface. The cortical surface was immediately covered with silicone oil. A more precise location of the primary auditory cortex was identified and later confirmed electrophysiologically (e.g., tuning, threshold, latency), as a region between the anterior and posterior ectosylvian sulci.

Acoustic stimuli

The stimuli used were pure tones, wide- and narrowband click trains with fixed inter-click intervals (ICI). The set of click-trains consisted of ICIs that were systematically varied from 3 to 100 ms. Typical ICIs were 3, 5, 7.5, 10, 12.5, 15, 20, 30, . . . 70, 75, 100 ms. Each click-train lasted for 600 or 1,000 ms. The wideband clicks were rectangular pulses 0.1 ms in width. This type of stimulus typically elicited responses from middle-layer A1 neurons under anesthetized conditions regardless of their characteristic frequency (CF). The narrowband clicks were sinusoids at a unit's CF whose amplitude was modulated by a Gaussian envelope. The widths of the Gaussian function were determined by the standard deviation parameter (a value of 0.2 was used for this study). The duration of these clicks was ~4 ms, measured where the modulation depths had decayed to $<$5% of its maximal depth. A sample waveform is shown in Fig. 6, *inset.* In terms of bandwidth, these clicks were ~1 kHz wide, measured where the Fourier magnitude had decayed to 5% of its maximal depth. Except at 3 ms ICI, there is no overlapping between successive clicks. This type of "Gaussian" click has previously been used in psychophysical experiments (Buell and Hafter 1988). The advantage of using narrowband clicks is that a stimulus' energy is concentrated on a neuron's excitatory receptive field, and the bandwidths of these clicks are comparable to a neuron's frequency receptive field. The majority of Q_{10} (CF/bandwidth at 10dB above threshold) values from Phillips and Irvine (1981) ranged from 4 to 16. Schreiner and Mendelson (1990) reported average Q_{10} values of 4.28–5.39. Assuming Q_{10} of 5 for neurons with CFs ranging from 1 to 20 kHz, this corresponds to bandwidths of 0.2–4.0 kHz. Unlike rectangular clicks, Gaussian clicks are less likely to activate inhibitory sidebands that typically flank an A1 neuron's excitatory receptive field (Brosch and Schreiner 1997; Phillips 1988; Schreiner and Sutter 1992; Shamma et al. 1993; Suga 1965).

All acoustic stimuli were delivered under free-field conditions by a speaker located 3 ft in front of the animal. The speaker (XTS-35, Radio Shack) had a flat (±5 dB) frequency response from 100 Hz to 20 kHz. Stimuli were generated digitally on a computer at full range of a 16-bit D/A converter at 50-kHz sampling rate and attenuated to desired sound pressure level (DA3, PA4, Tucker-Davis Technologies). Gaussian clicks were additionally low-pass filtered at 25 kHz

(3382 Filter, Krohn-Hite). Stimuli from each stimulus set were presented in random order. Click stimuli were typically presented at 60 dB SPL for 20 repetitions for all units. In some units, several sound levels were tested for click stimuli. Inter-stimulus intervals were ~1 s in duration.

Recording procedure

All recording experiments were conducted with the animal placed in an anechoic chamber (Industrial Acoustics Company). The interior of the chamber was covered by 3-in acoustic absorption foam (Sonex, Illbruck). Extracellular recordings were made using tungsten microelectrodes (Microprobe; BAK Instrument) with impedances typically ~1.5–2.5 MΩ at 1 kHz. For each cortical site, the electrode was placed perpendicularly to the cortical surface and advanced to a depth of 600–800 μm underneath the cortical surface, corresponding to cortical layers 3b and 4. The CF and threshold were identified using a manually controlled oscillator (4300B, Krohn-Hite) and attenuator. Click stimuli were then presented in random order. Neural activity was amplified and filtered at 0.3–7 kHz. Action potentials were sorted by a window discriminator (SD1, Tucker-Davis Technologies) or a template-matching spike sorter (MSD, Alpha Omega Engineering). In this report, we conservatively labeled all units as multi-units. The primary auditory cortex was systematically sampled from dorsal to ventral regions as conditions permitted.

Data analysis

Data were initially examined with dot raster plots and poststimulus time histograms. Temporal discharge patterns produced by click stimuli were classified into three regions: stimulus-synchronized (at long ICIs), nonsynchronized (at intermediate ICIs), and oscillatory or rate-change (at short ICIs). Quantitative measures were applied to calculate the boundaries separating these regions. For stimulus-synchronized responses (excluding onset responses to the click train), a mean vector strength, $\bar{R}$, was computed from the following formulae (Goldberg and Brown 1969):

$$\bar{R} = \frac{1}{n}\sqrt{x^2 + y^2} \quad x = \sum_{i=1}^{n} \cos\,\theta_i \quad y = \sum_{i=1}^{n} \sin\,\theta_i \quad \theta_i = 2\pi\,\frac{t_i}{T}$$

where n is the total number of spikes, t_i is the time of spike occurrence, and T is the inter-click interval. Rayleigh statistics, $2n\bar{R}^2$, were then calculated to determine the significance of the stimulus-synchronized response (Buunen and Rhode 1978; Mardia and Jupp 2000; Shofner et al. 1996). Two values of the Rayleigh statistic were calculated for each ICI using the first and second halves of the response. To ensure that the synchronized response was sustained throughout the stimulus duration, the minimum of the two statistics at each ICI was used in the determination. The *synchronization boundary* was calculated from the minimum Rayleigh statistic-versus-ICI curve with a two-step analysis. First, an estimate of the synchronization boundary was obtained using a threshold value of 13.8, which corresponds to a P value of 0.001 for the Rayleigh test (Mardia and Jupp 2000). This estimated boundary ICI was the minimum ICI with all longer ICIs showing significant synchronization. Then a second-order polynomial was fit locally (5 points) around the estimated threshold. The ICI where the fitted line crossed the Rayleigh threshold was taken as the synchronization boundary. For units that showed a change in firing rate with ICI, the total discharge rates of response between 50 and 200 ms after stimulus onset were calculated at each ICI. Similar to the synchronization boundary calculation, a local second-order polynomial fit (5 points) was done, and a threshold, equal to 25% of the range of response rates (maximum rate – minimum rate), was determined. The ICI at which the fitted polynomial crossed the rate threshold was taken as the *rate-change boundary*. All statistical tests between sets of boundary distributions were done using Wilcoxon rank sum tests of significance (Rice 1988).

RESULTS

General observations

Data reported here were based on 175 units recorded from eight cats (mostly left hemisphere A1). The sampled units covered a wide range of CFs (1–20 kHz) and locations along the dorsal-ventral axis. Because no significant differences were found in our analyses between data obtained under pentobarbital-sodium and ketamine anesthesia, the results reported here combined all studied units from both conditions. Several representative examples of responses to click train stimuli are given in Fig. 1. Usually, the onset responses were similar across ICIs. What differentiates responses to click trains with different ICIs were the discharges induced by later clicks. In general, three classes of temporal discharge patterns were observed in response to click train stimuli: *stimulus-synchronized discharges*, *stimulus-induced oscillatory discharges*, and *nonsynchronized discharges*. The majority of units we studied (74%) exhibited significant stimulus-synchronized discharges at long ICIs. Stimulus-synchronized discharges can be seen in areas labeled with "I" in Fig. 1, *A–C*. The strength of response synchrony differed from unit to unit as did the shortest ICI at which discharges are synchronized to clicks. As the ICI is shortened, the ability of a unit to synchronize to stimuli begins to degrade. Stimulus-synchronized discharges are clearly present at ICIs >25 ms for the unit in Fig. 1*A*. No significant response synchrony exists at ICIs shorter than 40–50 ms for the units shown in Fig. 1, *B* and *C*. A very small number of units showed synchronized discharges to ICIs shorter than 10 ms (data not shown, see DISCUSSION). Quantitative measures of the boundary at which response synchrony disappears will be discussed in later sections.

Another stimulus-induced discharge pattern is the oscillation evoked by click trains with short ICIs usually <20 ms (marked as "III" in Fig. 1*B*). The frequency of the oscillation was typically at 8–12 Hz, did not change significantly as ICI changed, and was clearly unrelated to the repetition rate of a click train. The coherence of the oscillation decays as time progresses after stimulus onset. Such oscillatory responses in the auditory cortex have been previously reported (Schreiner and Urbas 1986) and are thought to result from thalamocortical loops (e.g., Eggermont 1992). This oscillation was only observed in a subset of cortical units that we studied (11%).

One type of nonsynchronized firings (after responses to the 1st click) is nearly random discharges at intermediate ICIs as illustrated in Fig. 1, *B* and *C* (labeled with "II"). At ~20–30 ms ICI, the response beyond the initial onset is undifferentiated from spontaneous activity. The firing rate was generally observed to be approximately the same as or slightly higher than spontaneous activity. Typically there was a range of ICIs at which such firings were observed. The majority of units exhibited this kind of firing property whether or not they had synchronized activity at longer ICIs.

The other type of nonsynchronized firings was observed at the shortest ICIs tested (usually <10 ms) where some units responded to click trains with a brief cluster of discharges whose magnitude decreases as ICI increases (labeled with "III" in Fig. 1*D*). This increased firing occurred 50–200 ms after the stimulus onset. We

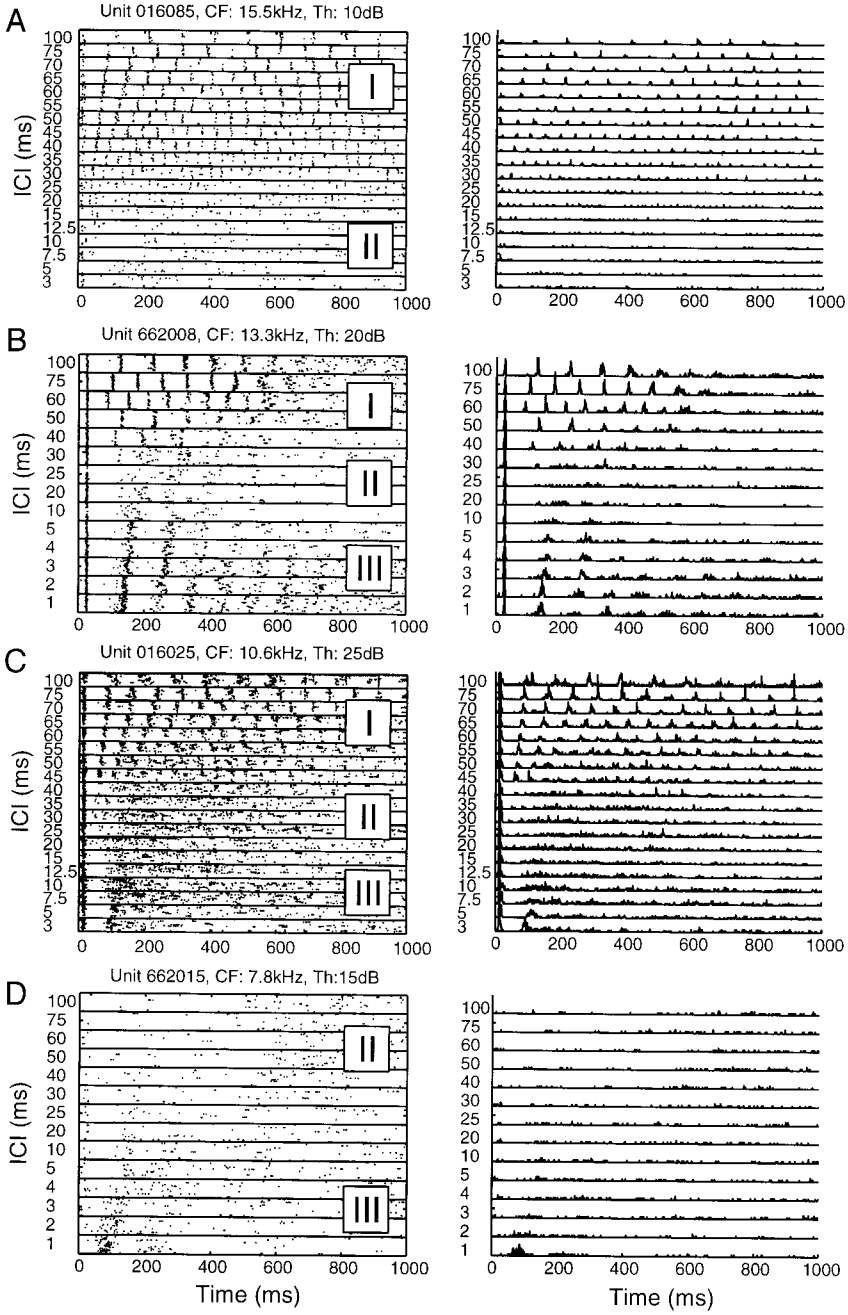

FIG. 1. Representative examples of different temporal discharge patterns in response to click stimuli. *Left*: dot raster plots; *right*: the corresponding poststimulus histogram (PSTH). The vertical axis represents the inter-click interval (ICI) of the stimulus, and the horizontal axis is time. Click trains at each stimulus ICI were presented 20 times in randomized order. Different regions of temporal discharge patterns are marked by I (synchronized activity), II (nonsynchronized activity), and III (oscillation or rate-change). *A*: a unit with synchronization responses at long ICIs (I). The stimulus-synchronized response stopped at 25 to 30-ms ICI. *B*: a unit showing both synchronization at long ICIs (I) and stimulus induced oscillations at short ICIs (III). Notice that the oscillation frequency (~10 Hz) is largely independent of stimulus ICI. *C*: a unit showing synchronization at long ICIs (I) and rate-change response at short ICIs (III). The rate-change response occurred within a 50- to 200-ms window. *D*: a unit showing rate-change response at short ICIs (III), but not stimulus-synchronized response at long ICIs. Nonsynchronized discharges at medium and long ICIs can be seen in *A–D* (II).

encountered this type of response in ~25% of the units we studied. What distinguished this rate response from the response elicited by pure tones was the longer latency—about 50–100 ms versus 10–15 ms for tones—and the longer duration of the response. Sometimes this type of rate change was observed in units that also exhibit stimulus-synchronized firings at long ICIs (Fig. 1*C*).

Based on properties discussed in the preceding text, we divided the responses to tested ICIs into three regions (from long ICIs to short ICIs): responses to the long ICIs that produced stimulus-synchronized responses is referred to as *region I*; the responses to medium ICIs that produced nonsynchronized discharges is referred to as *region II*; and the third response type at short ICIs is referred to as *region III(osc)* for the oscillation or *region III(rate)* for the rate-change response. These regions are denoted on the dot raster plots in Fig. 1. An A1 unit may display one, two, or three of these regions in its responses to click stimuli.

Temporal and rate measures

Cortical responses to click train stimuli were quantified by average discharge rate or by Rayleigh statistics if stimulus-induced synchronization was present. Figure 2*A* shows typical Rayleigh statistic versus ICI curves for units that had well-defined stimulus-synchronizing characteristics. For these units, the Rayleigh statistic generally increases with increasing ICI, sometimes reaching a plateau at long ICIs. Most of the units shown here were not able to synchronize to the very fast temporal modulations present in the stimuli with the shortest

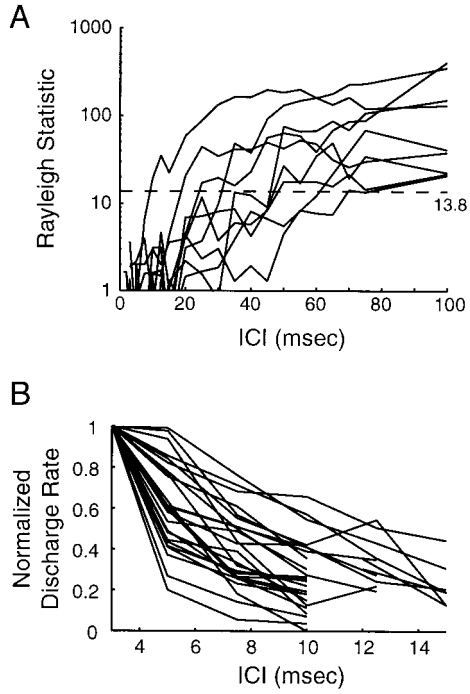

FIG. 2. Quantitative measures of temporal response properties. *A*: the Rayleigh statistic (see METHODS) calculated at each stimulus ICI is plotted (on a logarithmic scale) against the stimulus ICI for a number of representative units. The Rayleigh statistic typically increased as the ICI is increased, indicating that the temporal following response was stronger at longer values of ICI. The dashed line indicates statistical significance for the Rayleigh test. *B*: the average discharge rates were calculated with a window of 50–200 ms for each ICI and then normalized by the rate at 3 ms. The rates typically decreased monotonically with increasing stimulus ICI for units showing rate-change response. The curves show that there is a quantifiable change in discharge rate as a result of changing the ICI of click trains.

ICIs. Except for a small number of units, the Rayleigh statistic of most units decline to an insignificant level at ICIs less than ~20–40 ms.

Figure 2*B* shows the normalized total discharge rate plotted against ICI for those units that display rate changes at short ICIs. Discharge rate at each ICI is computed at 50–200 ms and normalized to the rate at the shortest ICI (3 ms). As ICI increases, the discharge rate drops off quickly. These curves suggest that it may be possible for these units to encode short ICIs with rate changes.

Distribution of boundaries between regions of distinct discharge patterns

Based on the measures shown in Fig. 2, boundaries that separate the three discharge regions were calculated for each unit. The synchronization boundary (separating regions I and II) specifies the minimum ICI below which the stimulus-synchronized response is no longer significant. This corresponds to the intuitive notion of temporal features of stimuli explicitly represented by temporal patterns of discharge. The rate-change boundary [separating regions II and III(rate)] specifies the maximum ICI above which a change in the firing rate of the unit is no longer detectable with respect to ICI.

SYNCHRONIZATION BOUNDARY. Distributions of synchronization boundaries based on data from two representative experiments are shown in Fig. 3, *A* and *C*. Each unit appearing in the histogram is capable of temporally representing any stimulus ICI greater than its boundary value. The median synchronization boundaries for these two experiments are 39.3 ms ($n = 57$) and 26.8 ms ($n = 49$), respectively. The distributions of the synchronization boundary cover a wide range of stimulus ICIs, with 25–75th percentile ranges of 26.0–57.9 ms and 13.4–50.1 ms, respectively. Figure 4*A* summarizes synchronization boundaries from all experiments. The median synchronization boundary calculated from the pooled data were 39.8 ms ($n = 131$) with the 25–75th percentile range of 20.4–58.8 ms. Therefore the stimulus rate that at least half of A1 units can follow with time-locked discharge patterns is ~25 Hz.

RATE-CHANGE BOUNDARY. Figure 3, *B* and *D*, shows distributions of rate-change boundaries for two individual experiments. The units included in the histogram have potential to code for those stimulus ICIs that are smaller than their boundary values using their discharge rate. The distribution of the pooled data are shown in Fig. 4*B*. It has a median value of 6.3

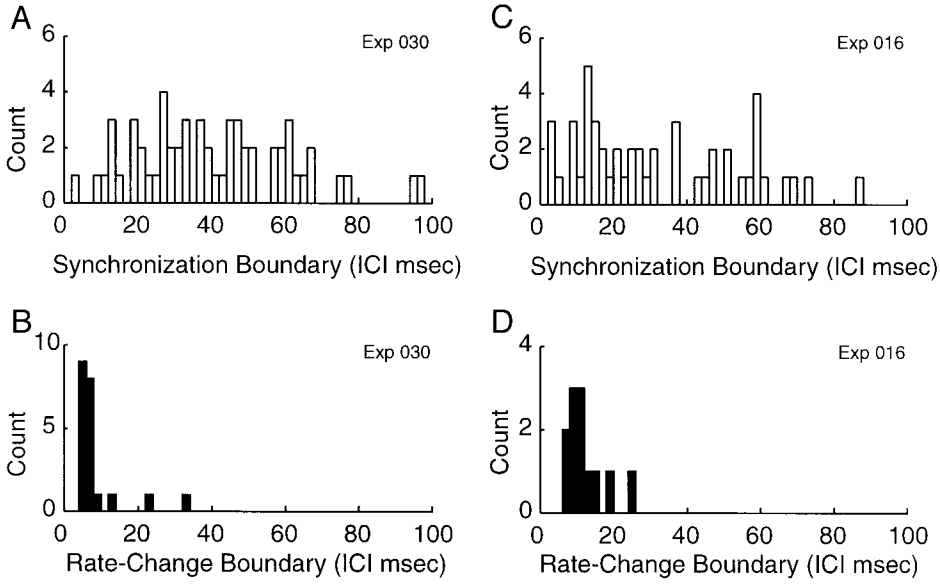

FIG. 3. Response boundaries from 2 representative experiments. *A*: distribution of synchronization boundaries of *experiment 030* (median = 39.3 ms [25%, 75%] = [26.0, 57.9] ms, $n = 57$). *B*: distribution of rate-change boundaries for *experiment 030* (median = 6.3 ms [25%, 75%] = [5.4, 7.4] ms, $n = 21$). *C*: distribution of synchronization boundaries for *experiment 016* (median = 26.8 ms [25%, 75%] = [13.4, 50.1] ms, $n = 49$). *D*: distribution of rate-change boundaries (median = 10.8 ms [25%, 75%] = [9.2, 13.9] ms, $n = 12$).

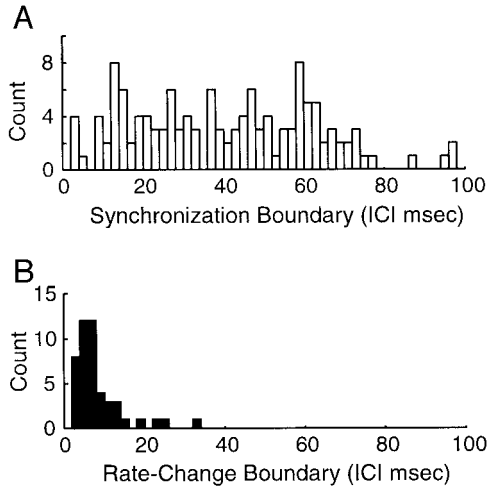

FIG. 4. Response boundaries from pooled data of all experiments. *A*: synchronization boundaries (median = 39.8 ms [25%, 75%] = [20.4, 58.8] ms, $n = 131$). *B*: distribution of rate-change boundaries (median = 6.3 ms [25%, 75%] = [5.2, 9.7] ms, $n = 47$).

ms ($n = 47$) and a 25–75th percentile range of 5.2–9.7 ms. Both individual experiments and the pooled data have similar distributions.

Effect of sound intensity

In a subset of units that exhibited strong stimulus-synchronized responses, we also tested the robustness of the synchronization boundary to sound-level changes. Invariance to changes in sound pressure level would further support the notion that this boundary is an intrinsic property to an A1 neuron and is independent of external stimulus. The thresholds of the units to pure tones were typically well below the 60 dB SPL we used for most click stimuli. The sensitivity of the synchronization boundary was examined at 20 dB lower than this standard sound level. The majority of units showed a decrease in firing rate to click stimuli at this lower sound level, 40 dB SPL (data not shown), indicating that the firing rates of these units were not saturated for the SPL range tested. There were no significant changes in the median synchronization boundaries as a function of SPL as shown by data in Fig. 5*A*. The distributions of synchronization boundaries were not significantly different ($P = 0.14$, Wilcoxon rank sum) between the two sound levels (40 dB SPL: median = 30.8 ms [25%, 75%] = [21.4, 42.1] ms, $n = 20$; 60 dB SPL: median = 39.3 ms [25%, 75%] = [26.0, 57.9] ms, $n = 57$). Figure 5*B* compares the results of changing SPL on a unit-by-unit basis for those units that were presented with click stimuli at both 40 and 60 dB SPL. Most points fall near the diagonal line indicating that there is a high degree of correlation between the synchronization boundaries at the two sound levels. Therefore moderate changes in sound level did not seem to significantly alter the synchronization boundary.

The difference in the rate-change boundary distributions was not significant ($P = 0.18$, Wilcoxon rank sum) between the two sound-levels (40 dB: median = 7.3 ms [25%, 75%] = [6.3, 12.1] ms, $n = 5$; 60 dB: median = 6.3 ms [25%, 75%] = [5.4, 7.4] ms, $n = 21$; Fig. 5*C*). We had only a few units that showed rate changes and for which we were able to record responses at both 40 and 60 dB. For these units, the rate-change boundary was similar at both sound levels, as shown in Fig. 5*D*. These data suggest that the rate-change boundary was largely independent of moderate changes in sound level.

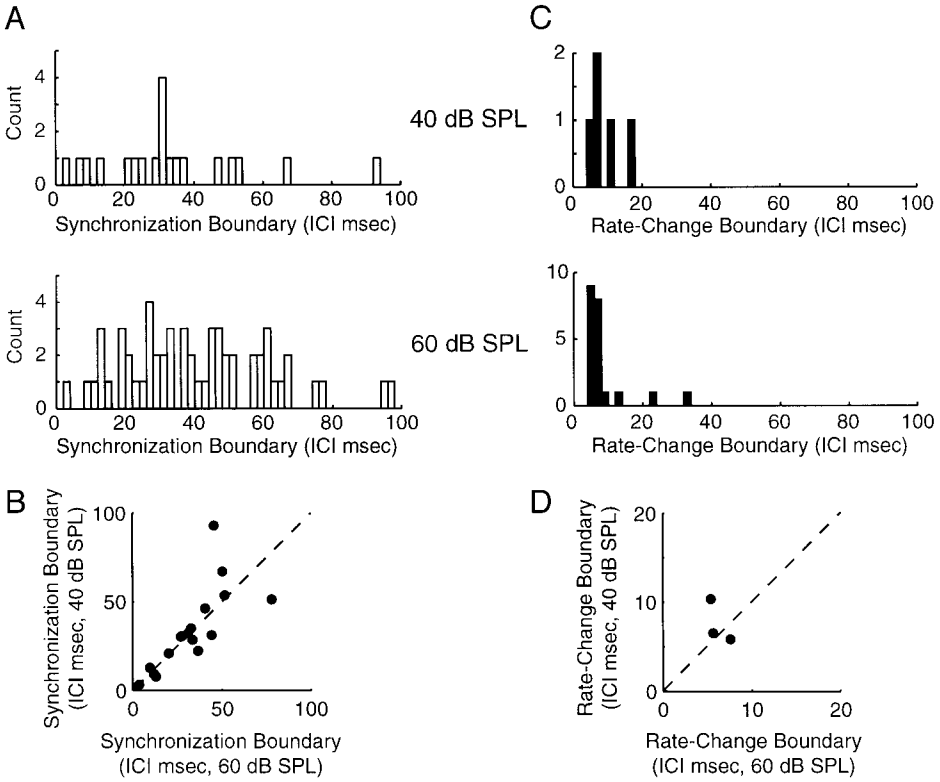

FIG. 5. Effect of sound level on response boundaries. *A*: distributions of synchronization boundaries at 2 different stimulus sound levels. The distribution of synchronization boundaries at 40 dB SPL is not significantly different ($P = 0.14$, Wilcoxon rank sum) from the distribution at 60 dB SPL (40 dB SPL: median = 30.8 ms [25%, 75%] = [21.4, 42.1] ms, $n = 20$; 60 dB SPL: median = 39.3 ms [25%, 75%] = [26.0, 57.9] ms, $n = 57$). *B*: synchronization boundaries for the 60 and the 40 dB SPL were plotted against each other for each cortical site on a unit-by-unit basis. *C*: distributions of rate-change boundaries at 40 and 60 dB SPL (40 dB: median = 7.3 ms [25%, 75%] = [6.3, 12.1] ms, $n = 5$; 60 dB: median = 6.3 ms [25%, 75%] = [5.4, 7.4] ms, $n = 21$). *D*: comparison of rate-change boundary on a unit-by-unit basis.

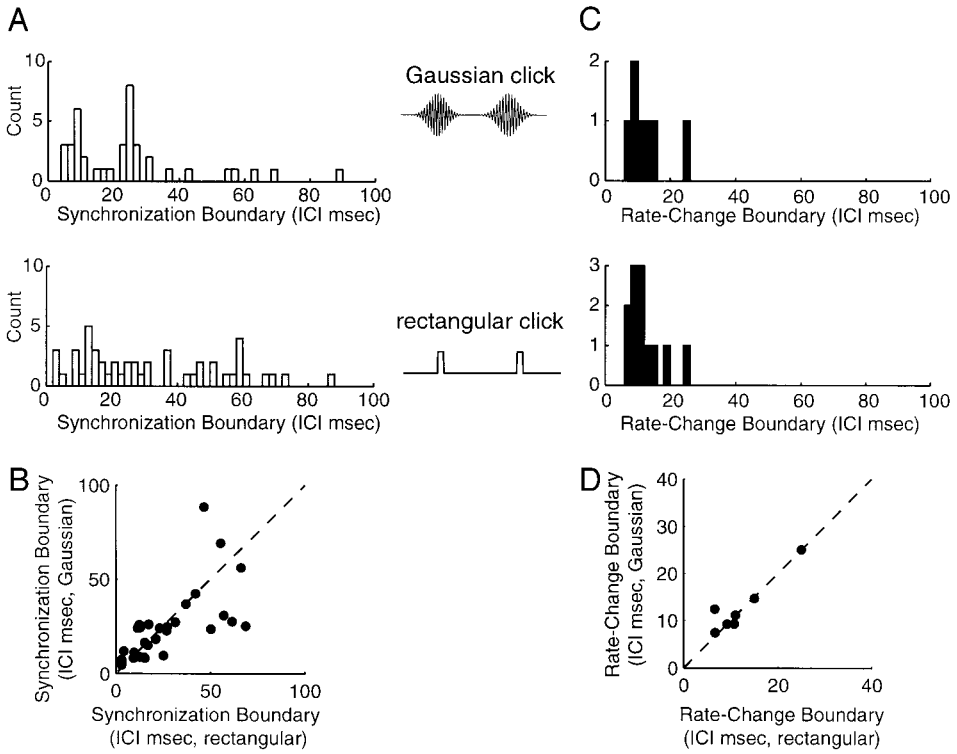

FIG. 6. Effect of stimulus bandwidth on response boundaries. Format is similar to Fig. 5. *A*: boundary distributions for Gaussian clicks and rectangular clicks (Gaussian: median = 24.1 ms [25%, 75%] = [8.9, 27.3] ms, $n = 40$; rectangular: median = 26.8 ms [25%, 75%] = [13.4, 50.1] ms, $n = 49$). No significant differences ($P = 0.09$, Wilcoxon rank sum) resulting from the 2 stimulus conditions are apparent. *B*: the boundaries resulting from Gaussian clicks are plotted against the boundary resulting from rectangular clicks on a unit-by-unit basis. *C*: distributions of rate-change boundaries for Gaussian and rectangular clicks (Gaussian: median = 11.1 ms [25%, 75%] = [9.3, 14.1] ms, $n = 7$; rectangular: median = 10.8 ms [25%, 75%] = [9.2, 13.4] ms, $n = 12$). *D*: comparison of rate-change boundary on a unit-by-unit basis.

Comparison between wideband and narrowband clicks

An important factor that can significantly shape responses to click stimuli is the lateral inhibition that has been known to flank excitatory receptive fields of most A1 neurons (Brosch and Schreiner 1997; Phillips 1988; Schreiner and Sutter 1992; Shamma et al. 1993; Suga 1965). The data presented in Figs. 1–5 were obtained with rectangular clicks ("wideband clicks"), a class of signals whose broad spectrum is likely to activate inhibitory sidebands. Wideband clicks are commonly used in neurophysiological experiments because they can easily evoke responses from neurons with all CFs. To help dissect the contribution of excitatory and inhibitory mechanisms, we applied in this study a class of narrowband clicks called "Gaussian" clicks. The band-limited spectral characteristics of this stimulus can significantly reduce the contribution of lateral inhibition. It was expected that if lateral inhibition shaped the temporal response, the use of Gaussian clicks would lessen the effect. However as shown in Fig. 6*A*, the distributions of synchronization boundaries were not significantly different ($P = 0.09$, Wilcoxon rank sum) between responses to Gaussian clicks (median = 24.1 ms [25%, 75%] = [8.9, 27.3] ms, $n = 40$) and rectangular clicks (median = 26.8 ms [25%, 75%] = [13.4, 50.1] ms, $n = 49$). Figure 6*B* further compares the synchronization boundaries between Gaussian and rectangular clicks on a unit-by-unit basis. These data suggest that lateral inhibitions do not play a significant role on the stimulus-following ability of A1 units in this preparation.

We also examined the effect of stimulus bandwidth on the rate-change boundary (Fig. 6, *C* and *D*). No significant differences ($P = 0.71$, Wilcoxon rank sum) were found between the response distribution for the two stimulus types for the rate change boundary (Gaussian: median = 11.1 ms [25%, 75%] = [9.3, 14.1] ms, $n = 7$; rectangular: median = 10.8 ms [25%, 75%] = [9.2, 13.4] ms, $n = 12$). When the rate-change boundary is plotted on a unit-by-unit basis for responses to the two click types, most points fall near the diagonal line. This indicates that the rate-change boundary was not significantly affected by stimulus bandwidth.

Correlation to response latency

We calculated minimum latencies to the initial click of click trains with ICIs >30 ms. In Fig. 7, the synchronization boundaries are plotted against these values. Although the correlation is loose, there seems to be a trend in the data with shorter latency units giving smaller boundary values. If the units in Fig. 7 are split into two sets according to their latency (≤11 and >11 ms), then the synchronization boundaries of these two

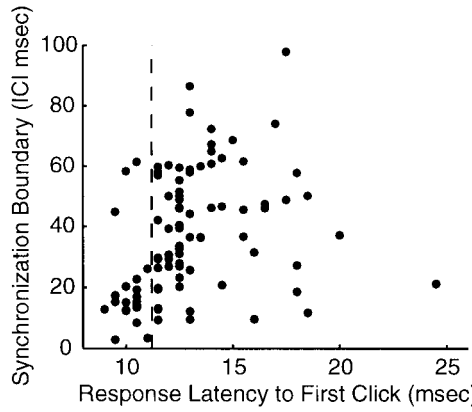

FIG. 7. Correlation of synchronization boundary and response latency. Average latency values ($n = 93$) were calculated from the response to the first click of each click train (ICIs >30 ms). Units with ≤11-ms latency (- - -) had, on average, smaller synchronization boundaries than units with latencies >11 ms. This difference in boundary distributions between these 2 groups of units is significant ($P \ll 0.01$, Wilcoxon rank sum).

groups are significantly different ($P \ll 0.01$, Wilcoxon rank sum) from each other. There is a significant shift in synchronization boundary distribution that depended on latency. The trend is consistent with the prediction one would make from a simple neuron model, i.e., the shorter the integration period of a neuron, the shorter its response latency and consequently, the faster its ability to synchronize to successive stimuli.

DISCUSSION

Comparison with previous studies

Most previous studies on cortical responses to successive stimuli using click trains or amplitude-modulated (AM) sounds have focused on modulation transfer functions, and in particular, the best modulation frequency (BMF) (Eggermont 1994, 1998, 1999; Gaese and Ostwald 1995; Schreiner and Urbas 1986, 1988). As our purpose in this study is to investigate the representation of rapidly modulated stimuli, the repetition rate (or modulation frequency in a more general sense) of our click stimuli ranged from 10 Hz (typically the BMF reported in previous studies) to 333 Hz (3-ms ICI). In comparison, modulation frequencies used in most previous studies ranged from 1 to ~100 Hz. The synchronization boundary calculated in our study is frequently referred to in the literature as the limiting rate (of stimulus-synchronized responses).

Previous studies have found limiting rates of A1 neurons to be typically <20 Hz in anesthetized preparations (Eggermont 1998; Gaese and Ostwald 1995; Phillips et al. 1989; Schreiner and Urbas 1988), and as high as >100 Hz in unanesthetized animals (de Ribaupierre et al. 1972; Goldstein et al. 1959). There is a wide variation in the reported limiting rates as well as in the criterion for defining the limiting rate. Recordings of single units in unanesthetized animals by de Ribaupierre et al. (1972) found the median limiting rate of their data to be between 50 and 100 Hz with an exceptional unit whose limiting rate was as high as 1,000 Hz. Creutzfeldt et al. (1980) recorded simultaneously from thalamic and cortical neurons of unanesthetized guinea pigs and computed modulation transfer functions based on the response amplitude at steady state to tone pulses (trapezoidal modulation) in relation to the amplitude of the response to the first tone pulse. They reported that the steady-state amplitude of the response ($n = 12$) dropped to 50% when the modulation frequency was 25 Hz and to 25% at ~50 Hz. In contrast, the synchronization boundaries that Phillips et al. (1989) found were almost all <10 Hz using a series of tone pulses at the CF of the neuron and a criterion that defined the limiting rate as 85% entrainment of spikes to the click. In the study by Eggermont (1998), the limiting rates (50% of maximum magnitude of BMF) due to clicks were found to be clustered normally ~9–12 Hz with no significant differences due to cortical area or single versus multiple unit recordings. The variability of limiting rates that are reported by these studies is quite large, ranging from ~8 up to 100 Hz.

The variation in these previous studies was attributed in large part to the analytical method used (Eggermont 1991), although it should be pointed out that some of these differences in limiting rates were likely introduced by different types of repetitive or periodic stimuli. Using entrainment rather than vector strength in analysis may result in different values for limiting rates. With a single set of data, Eggermont (1991) explored the effects of various analytical techniques on the limiting rate, which was defined in that study as 50% of maximum of the particular measure used. The results varied from 3 Hz using a rate calculation rMTF/click to 24 Hz for a vector strength (most similar to ours) to >32 Hz for rMTF/train. The different analytical techniques could account for part of the variation in the findings of the studies mentioned. Given the wide variation in reported limiting rates, our data on the synchronization boundary, with an median limiting rate of ~25 Hz (equivalent to ~40 ms ICI), are within range of published data using anesthetized preparations.

Occasionally, we encountered a few units that had exceptionally low synchronization boundary (~10 ms). These units did not show evidence of suppression after the initial click that was typically seen in most A1 units we studied, and they usually had particularly short response latency (<10 ms). We suspect that these rare units may be recorded directly from afferent thalamocortical inputs. It is also possible that these highly synchronized responses were due to multi-unit recordings. Our impression is that multi-unit recordings tend to display a higher degree of response synchrony than single-unit recordings.

Because response latency provides an indication of temporal integration time, a neuron's latency may be correlated with its stimulus-synchronizing ability. In our results, we found that the synchronization boundary was loosely correlated with response latency. A similar covariation of latency with BMF has been reported in the inferior colliculus of the cat (Langner et al. 1987). The precision of the cortical neurons' responses to transients with respect to the first spike latency has been shown to be only slightly worse than in the auditory nerve (Heil and Irvine 1997; Phillips and Hall 1990). The precision of the first spike latency at the cortical level appears to be enough to support entrainment to very short ICIs (Phillips 1989) but it does not explain the low entrainment rates in this and previous studies. It is important to note that the timing information that Phillips reported was only for onset responses. Other factors besides spike timing can reduce entrainment (Phillips 1989). The minimum response latency in the cortex can be relatively precise, and it is reasonable to expect that the stimulus-synchronizing ability of these neurons can also be high since there would be less overlap in the responses to successive stimuli. The loose correlation between a unit's synchronization boundary and its first spike latency indicates that temporal integration plays a role in shaping the synchronized response but at the same time, suggests that there must be other factors that limit the unit's stimulus-synchronization ability.

An important difference between our study and previous studies employing click and AM stimuli is that we investigated cortical responses to click trains with very short ICIs. We identified in this study rate-change responses that occurred in a subset of A1 units when stimulated by click trains with ICIs <10–15 ms. This phenomenon has not been reported in previous studies because our maximum repetition rate (or equivalently, modulation frequency) was higher than in most previous studies. For example, maximum repetition rate was 64 Hz (16 ms ICI) in Eggermont (1998). Although de Ribaupierre et al. (1972) did use click train rates up to 3,000 Hz, the number of cortical units sampled was relatively small in that study. In the present study, a small, but significant number of units displayed rate-change property (25%), out of a large sample

size of 175 units. We tested the entire range of ICIs (3–100 ms) in each of these recorded units.

Finally, it is important to point out that the results of the present study were based on recordings made from middle-layers of A1, which are active under the anesthetics used. Future studies need to further investigate response properties of upper layer neurons to these repetitive stimuli, presumably under unanesthetized conditions.

Effects of stimulus bandwidth and its implications

The fact that changing the bandwidth of our click stimuli did not significantly alter the synchronization boundary indicates that lateral inhibition is not a significant factor in shaping the temporal response to successive stimuli, at least in anesthetized preparations. This result is supported by observations from previous studies. de Ribaupierre et al. (1972), in addition to clicks, also tested a train of noise bursts, 1–2 ms duration for each burst. Although clicks are considered wideband stimuli, they contain regions in their spectrum where the amplitude is nearly zero. Noise bursts, on the other hand, have a more evenly distributed spectrum. de Ribaupierre et al. (1972) did not note any significant differences in the limiting rate between the noise bursts and the click trains, although their sample size was small ($n = 7$). Schreiner and Urbas (1988) reported that the modulating envelope shape (rectangular AM vs. sinusoidal AM) had little influence on the temporal-following ability in terms of BMF. The evidence suggests that the excitatory mechanisms, namely temporal integration by an A1 neuron, may play a primary role in shaping stimulus-synchronized responses. Another mechanism that may have significant influence on responses to successive stimuli is on-CF inhibition. Responses to single click (or the initial click in a click train), whether wide- or narrowband, almost always produced a prolonged period of inhibition (see examples in Fig. 1), which is similar in nature to the inhibition evoked by a brief CF tone burst. Dissecting the contribution of on-CF inhibition from temporal integration will require other experimental manipulations and needs be investigated in future studies.

Effect of anesthetics

Two types of anesthetics were used in our experiments, ketamine and pentobarbital sodium. There appeared to be no significant differences in the response boundaries we characterized under both anesthetic conditions, although spontaneous activity was higher under ketamine than under pentobarbital-sodium condition. A previous report indicated that anesthetics have a suppressive effect on the stimulus-following responses of cortical neurons (Goldstein et al. 1959). It found that in the same animals click-following responses of evoked cortical potentials were limited to ~100 Hz under pentobarbital sodium or Dial anesthesia and ~200 Hz when the animals were unanesthetized. Anesthetics may reduce the efficacy of the temporal integration mechanism and prolong inhibition, both of which can contribute to a reduced stimulus-following capacity (Goldstein et al. 1959). The exact mechanisms on how the anesthetic operate are yet unknown. The other side effect of anesthetics may be the 8-to 10-Hz intrinsic oscillations seen in this and a number of previous studies (Eggermont 1992; Schreiner and Urbas 1986, 1988). In contrast, de Ribaupierre et al. (1972) did not report intrinsic oscillations in awake cats. The range of repetition rate used in that study was approximately similar to ours. Despite these limitations of anesthetics, data obtained in this and previous studies serve as a basis for future studies under awake and behaving conditions. A rigorous comparison of cortical responses under both anesthetized and unanesthetized conditions using the same stimuli would provide important insight into fundamental mechanisms underlying temporal processing in the auditory cortex.

Representation of rapid inter-stimulus intervals

The limit on response synchronization found in this study poses a significant question as to how cortical neurons can represent information that is too rapid to be encoded explicitly by temporal discharge patterns. The results of this and other studies show that the majority of cortical neurons cannot follow temporal sequence of stimuli at rates greater than ~20–40 Hz. Thus if the cortex relies exclusively on the temporal discharge patterns of individual neurons to encode complex sounds that are rapidly modulated, it is expected that the fidelity of that representation would be poor. This hypothesis is, however, contradicted by demonstrated perceptual capabilities of humans and animals.

When the temporal discharge patterns of individual cortical neurons no longer follow the stimulus, an alternative coding scheme must be used. Our data suggest that the representation of rapid inter-stimulus intervals may be coded by a rate measure. This is consistent with data from Bieser and Muller-Preuss (1996) for sinusoidal amplitude modulated sounds. At very short stimulus ICIs, our results show that there is a population of neurons that is able to signal ICI changes by the discharge rates of the constituent neurons. This result suggests

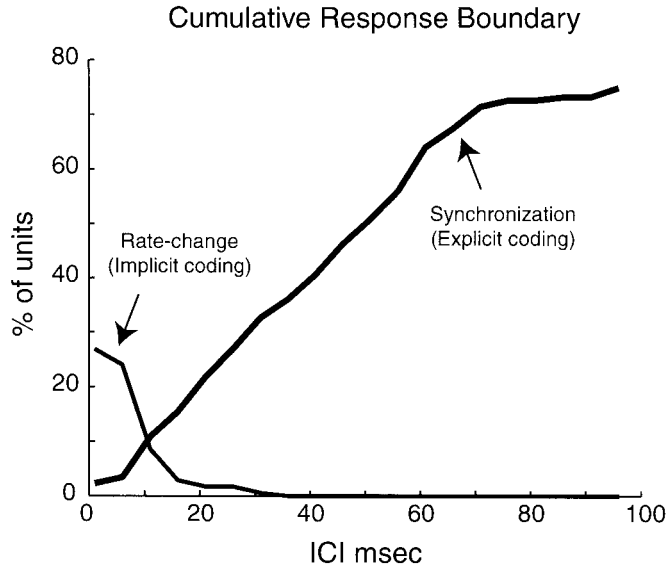

FIG. 8. A proposed 2-stage model for ICI representation. Curves are based on the data shown in Fig. 4. The thick line shows the percentages of units with synchronization boundaries less than or equal to each ICI. The thin line shows the percentages of neurons with rate-change boundaries greater than or equal to each ICI. At long ICIs, a large percentage of neurons that can represent the stimulus intervals explicitly by their temporal discharge patterns. For short ICIs, an implicit rate-code representation is suggested by the data.

that the representation of rapid repetitive stimuli has been transformed from an explicit temporal code to an implicit rate code at A1, possibly through both subcortical and cortical processing. The resultant representation of the stimulus by discharge rate may be correlated to the perceptual quality of such sounds as a single event rather than a series of discrete events (Hirsch 1959; Miller and Taylor 1948).

We considered the possibility that the rate-change responses we observed are due to spectral effects. While spectral effects cannot be completely ruled out, it does not seem to be a significant factor for several reasons. First, the rate-change boundary did not appear to be much affected by the click bandwidth. Since the narrowband Gaussian clicks are less likely (or to a smaller extent) to activate inhibitory sidebands than wideband clicks and both click types produce the same rate-change response, spectral effects due to inhibitory sidebands are minimal. Second, shortening the ICI of the click trains does not change the envelope of the power spectra only the magnitude. Since the envelopes of the power spectra have consistent shapes at each ICI, there are insufficient spectral cues for discrimination between different ICIs. We also observed that changing sound level did not seem to significantly alter the rate-change boundary. This suggests that the rate-change response was also largely independent of the greater power associated with shorter ICIs.

Temporal/rate-code model

Our findings suggest that a plausible model of representing sequential stimuli would consist of a combined temporal and rate representation. At longer ICIs, consistent with previous studies, sequential stimulus events can be coded explicitly by neuronal temporal discharge patterns. At shorter inter-stimulus intervals, our data suggest that the ICI can be represented implicitly by a rate code. If there is a sufficient overlap in ranges of ICIs represented by these two coding schemes, the combination should provide an adequate representation of the entire range of ICIs used in this experiment. We illustrate this two-stage model in Fig. 8. As ICI is shortened, the percentage of units able to explicitly represent the stimuli decreases. However, the percentage of units able to signal ICI changes increases. The model suggests that as the inter-stimulus interval becomes shorter, the cortical representation shifts from being predominantly explicit temporal coding to predominantly implicit rate coding. For the entire range of ICIs to be adequately represented, there should be a sufficient overlap between the response boundaries. In our samples, 74% of studied units exhibited stimulus-synchronized responses at some ICIs. Approximately 25% of these units can signal ICIs down to ~20 ms. At ICI equal to 10 ms, only 10% of units were able to represent this and other longer ICIs. A total of 25% of all units we studied showed rate-change responses at short ICIs, and 10% of all units could signal ICI changes ≤10 ms. Although the number of units is small, their existence, as revealed by the present study, supports the notion of a two-stage processing scheme. It remains to be seen whether the composition of the response patterns we identified using click stimuli changes under unanesthetized conditions. Nevertheless the model presented here is suggestive of the neural correlate of the perceptual change from discrete events to a sustained sound with increasing the stimulus repetition rate from 40 to 250 Hz (Miller and Taylor 1948), which is equivalent to 4 to 25-ms ICI.

We thank Dr. I. Bruce, Dr. R. Ramachandran, and D. Barbour for helpful comments on the manuscript and Dr. L. Liang for technical assistance.

This study was supported by Whitaker Foundation Research Grant RG-96-0268, National Institute on Deafness and Other Communication Disorders Grant DC-03180, and a grant from the National Organization for Hearing Research.

REFERENCES

BIESER A AND MULLER-PREUSS P. Auditory responsive cortex in the squirrel monkey: neural responses to amplitude-modulated sounds. *Exp Brain Res* 108: 273–284, 1996.

BROSCH M AND SCHREINER CE. Time course of forward masking tuning curves in cat primary auditory cortex. *J Neurophysiol* 77: 923–943, 1997.

BUELL TN AND HAFTER ER. Discrimination of interaural differences of time in the envelopes of high-frequency signals: integration times. *J Acoust Soc Am* 84: 2063–2066, 1988.

BUUNEN TJ AND RHODE WS. Responses of fibers in the cat's auditory nerve to the cubic difference tone. *J Acoust Soc Am* 64: 772–781, 1978.

CREUTZFELDT O, HELLWEG F-C, AND SCHREINER C. Thalamocortical transformation of responses to complex auditory stimuli. *Exp Brain Res* 39: 87–104, 1980.

DE RIBAUPIERRE F, GOLDSTEIN MH JR, AND YENI-KOMSHIAN G. Cortical coding of repetitive acoustic pulses. *Brain Res* 48: 205–225, 1972.

EGGERMONT JJ. Rate and synchronization measures of periodicity coding in cat primary auditory cortex. *Hear Res* 56: 153–167, 1991.

EGGERMONT JJ. Stimulus induced and spontaneous rhythmic firing of single units in cat primary auditory cortex. *Hear Res* 61: 1–11, 1992.

EGGERMONT JJ. Temporal modulation transfer functions for AM and FM stimuli in cat auditory cortex. Effects of carrier type, modulating waveform and intensity. *Hear Res* 74: 51–66, 1994.

EGGERMONT JJ. Representation of spectral and temporal sound features in three cortical fields of the cat. Similarities outweigh differences. *J Neurophysiol* 80: 2743–2764, 1998.

EGGERMONT JJ. The magnitude and phase of temporal modulation transfer functions in cat auditory cortex. *J Neurosci* 19: 2780–2788, 1999.

ERULKAR SD, ROSE JE, AND DAVIES PW. Single unit activity in the auditory cortex of the cat. *Bull Johns Hopkins Hosp* 99: 55–86, 1956.

GAESE BH AND OSTWALD J. Temporal coding of amplitude and frequency modulation in the rat auditory cortex. *Eur J Neurosci* 7: 438–450, 1995.

GOLDBERG JM AND BROWN PB. Response of binaural neurons of dog superior olivary complex to dichotic tonal stimuli: some physiological mechanisms of sound localization. *J Neurophysiol* 32: 613–636, 1969.

GOLDSTEIN MH JR, KIANG NY-S, AND BROWN RM. Response of the auditory cortex to repetitive acoustic stimuli. *J Acoust Soc Am* 31: 356–364, 1959.

HEIL P AND IRVINE DR. First-spike timing of auditory-nerve fibers and comparison with auditory cortex. *J Neurophysiol* 78: 2438–2454, 1997.

HIRSCH IJ. Auditory perception of temporal order. *J Acoust Soc. Am* 31: 759–767, 1959.

JOLIOT M, RIBARY U, AND LLINAS R. Human oscillatory brain activity near 40 Hz coexists with cognitive temporal binding. *Proc Natl Acad Sci USA* 91: 11748–11751, 1994.

JORIS PX AND YIN TCT. Responses to amplitude-modulated tones in the auditory nerve of the cat. *J Acoust Soc Am* 91: 215–232, 1992.

LANGNER G. Periodicity coding in the auditory system. *Hear Res* 60: 115–142, 1992.

LANGNER G, SCHREINER C, AND MERZENICH MM. Covariation of latency and temporal resolution in the inferior colliculus of the cat. *Hear Res* 31: 197–201, 1987.

MARDIA KV AND JUPP PE. *Directional Statistics.* New York: Wiley, 2000.

MILLER GA AND TAYLOR WG. The perception of repeated bursts of noise. *J Acoust Soc Am* 20: 171–182, 1948.

PALMER AR. Encoding of rapid amplitude fluctuations by cochlear nerve fibres in the guinea pig. *Arch Otorhinolaryngol* 236: 197–202, 1982.

PHILLIPS DP. Effect of tone-pulse rise time on rate-level functions of cat auditory cortex neurons: excitatory and inhibitory processes shaping responses to tone onset. *J Neurophysiol* 59: 1524–1539, 1988.

PHILLIPS DP. Timing of spike discharges in cat auditory cortex neurons: implications for encoding of stimulus periodicity. *Hear Res* 40: 137–146, 1989.

PHILLIPS DP AND HALL SE. Response timing constraints on the cortical representation of sound time structure. *J Acoust Soc Am* 88: 1403–1411, 1990.

PHILLIPS DP, HALL SE, AND HOLLETT JL. Repetition rate and signal level effects on neuronal responses to brief tone pulses in cat auditory cortex. *J Acoust Soc Am* 85: 2537–2549, 1989.

PHILLIPS DP AND IRVINE RF. Responses of single neurons in physiologically defined primary auditory cortex (A1) of the cat: frequency tuning and responses to intensity. *J Neurophysiol* 45: 48–58, 1981.

PLOMP R. Rate of decay of auditory sensation. *J Acoust Soc Am* 36: 277–282, 1964.

POLLACK, I. Asynchrony: the perception of temporal gaps within periodic auditory pulse patterns. *J Acoust Soc Am* 42: 1335–1340, 1967.

POLLACK I. Asynchrony II: perception of temporal gaps within periodic and jittered pulse patterns. *J Acoust Soc Am* 43: 74–76, 1968.

RICE JA. *Mathematical Statistics and Data Analysis*. Pacific Grove: Wadsworth and Brooks, 1988.

RONKEN D. Monaural detection of a phase difference between clicks. *J Acoust Soc Am* 47: 1091–1099, 1970.

SCHREINER CE AND MENDELSON JR. Function topography of cat primary auditory cortex: distribution of integrated excitation. *J Neurophysiol* 64: 1442–1459, 1990.

SCHREINER CE AND SUTTER ML. Topography of excitatory bandwidth in cat primary auditory cortex: single-neuron versus multiple-neuron recordings. *J Neurophysiol* 68: 1487–1502, 1992.

SCHREINER CE AND URBAS JV. Representation of amplitude modulation in the auditory cortex of the cat. I. The anterior auditory field (AAF). *Hear Res* 21: 227–241, 1986.

SCHREINER CE AND URBAS JV. Representation of amplitude modulation in the auditory cortex of the cat. II. Comparison between cortical fields. *Hear Res* 32: 49–63, 1988.

SHAMMA SA, FLESHMAN JW, WISER PR, AND VERSNEL H. Organization of response areas in ferret primary auditory cortex. *J Neurophysiol* 69: 367–383, 1993.

SHOFNER WP, SHEFT S, AND GUZMAN SJ. Responses of ventral cochlear nucleus units in the chinchilla to amplitude modulation by low-frequency, two-tone complexes. *J Acoust Soc Am* 99: 3592–3605, 1996.

STEINSCHNEIDER M, AREZZO J, AND VAUGHAN HG JR. Phase-locked cortical responses to a human speech sound and low-frequency tones in the monkey. *Brain Res* 198: 75–84, 1980.

SUGA N. Functional properties of auditory neurones in the cortex of echolocating bats. *J Physiol (Lond)* 181: 671–700, 1965.

WHITFIELD I AND EVANS E. Responses of auditory cortical neurons to stimuli of changing frequency. *J Neurophysiol* 28: 655–672, 1965.